

Observations on the permeation performance of solvent resistant nanofiltration membranes

D.F. Stamatialis^{a,*}, N. Stafie^a, K. Buadu^a, M. Hempenius^b, M. Wessling^a

^a University of Twente, Faculty of Science and Technology, Membrane Technology Group, P.O. Box 217, NL-7500 AE Enschede, The Netherlands

^b University of Twente, Faculty of Science and Technology, Materials Science and Technology of Polymers Group, P.O. Box 217, NL-7500 AE Enschede, The Netherlands

Received 15 September 2005; received in revised form 12 December 2005; accepted 17 December 2005

Available online 30 January 2006

Abstract

This work presents a systematic study of the influence of membrane–solvent–solute interactions on the permeation performance of solvent resistant nanofiltration (NF) membranes. Two different tailor-made composite membranes are prepared by dip coating of a polymer onto a polyacrylonitrile (PAN) support: a hydrophobic (using polydimethylsiloxane (PDMS) polymer) and a new hydrophilic (using polyethylene oxide (PEO)–PDMS–PEO tri-block copolymer). The transport of various pure solvents through the PAN/PDMS and PAN/PEO–PDMS–PEO composite membranes is studied showing a reasonably linear relation between the solvent permeability and the ratio of membrane swelling/solvent viscosity.

For the transport of sunflower oil/toluene mixtures through the PAN/PDMS composite membrane, the “apparent” viscosity inside the membrane and the membrane swelling seem to be the main parameters affecting the toluene transport. The oil/toluene system is ideal. Osmotic phenomena are observed which can be interpreted by the van’t Hoff osmotic pressure model. Furthermore, flux coupling between oil and toluene is significant resulting in rather moderate oil retention by the membrane (70–80%). The coupling between oil/toluene is stronger than between oil/hexane.

For the transport of tetraoctylammonium bromide (TOABr)/toluene mixtures through the PAN/PDMS membrane the phenomena are more complex. The system is non-ideal and no osmotic phenomena are observed. This can be correlated with the formation of ion-pairs of TOABr in toluene. Furthermore, the concentration polarization phenomena are significant resulting in low toluene fluxes and 100% retention of TOABr by the membrane.

© 2005 Elsevier B.V. All rights reserved.

Keywords: Solvent resistant nanofiltration membrane; Polydimethylsiloxane; Polyethylene oxide; Oil; Toluene; Tetraoctylammonium bromide

1. Introduction

In recent years, research field of solvent resistant nanofiltration (SRNF) has progressed and important contributions have been published [1–6]. Most of the studies stress the importance of membrane–solvent–solute interactions on the membrane permeation performance. The transport phenomena are complex, and often unique for a specific system, due to the wide range of solvent and solute properties (polarity, viscosity or surface tension) and membrane properties (chemistry and structure) [1]. Vankelecom et al. [1] reported that the flux of various solvents (polar and non-polar) through a laboratory-made PAN–poly(ester) (PE)/PDMS membrane is influenced by

the solvent viscosity and affinity with the membrane. Koops et al. [3] studied the permeation of various solutes in ethanol and *n*-hexane through cellulose acetate membranes and also concluded that the solute–membrane–solvent interactions are important for the mass transport. A similar conclusion was drawn by Bhanushali et al. [4] for the transport of organic dyes and triglycerides in polar and non-polar solvents through polyimide (STARMEMTM) and silicone type NF membranes. For the solvent/solute transport mechanism through the same polyimide membrane, Scarpello et al. [5] suggested that other effects besides sieving may be important as the same solute is rejected to a various extent in the presence of different solvents.

In previous work [2,7], we studied the transport of oil/hexane and polyisobutylene (PIB)/hexane mixtures through tailor-made PAN/PDMS composite membranes. In these studies, we investigated the effect of PIB molecular weight as well as of the PDMS cross-linking degree on the membrane permeation performance

* Corresponding author. Tel.: +31 53 4894675; fax: +31 53 4894611.
E-mail address: d.stamatialis@utwente.nl (D.F. Stamatialis).

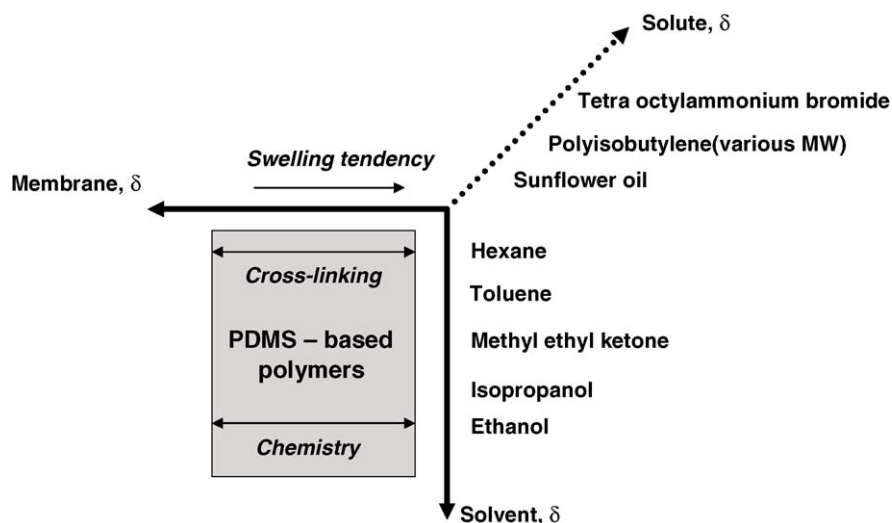


Fig. 1. Schematic presentation of the experimental strategy of this study.

(Fig. 1). For these systems the hexane permeability was influenced by an “apparent” viscosity inside the membrane and the membrane swelling. The solution diffusion model was applied to interpret the experimental results. The model falls short on the assumption that both solvent and solute permeate through the membrane in an uncoupled manner. The latter assumption seemed to be not valid since significant coupling phenomena between oil, PIB and hexane were observed.

In this work, we aim to extend the experimental evidence on mass transport phenomena of organic solvents and solutes through rubbery polymers. The research strategy is visualized in Fig. 1. In fact, we extend our experimental investigation into three different directions:

- I. By using suitable chemistry, we develop a new more hydrophilic separation layer material polyethylene oxide–PDMS–polyethylene oxide (PEO–PDMS–PEO). We prepare composite membranes and investigate the transport of various solvents (ethanol, isopropanol, methylethylketone, toluene, hexane) through it in comparison to the hydrophobic PAN/PDMS membrane (Fig. 1). This comparison is expected to show directly the effect of the membrane–solvent interactions on the membrane permeation performance.
- II. The transport of oil/toluene mixtures through the original PAN/PDMS composite membrane is studied. In comparison to previous work performed with oil/hexane [2,7], we keep the same membrane and solute but we change the solvent to toluene.
- III. The transport of tetraoctylammonium bromide (TOABr)/toluene mixtures through the PAN/PDMS composite membrane is studied. In comparison to the oil/toluene mixture (part II), the TOABr/toluene system is particularly interesting because previous work for the transport through a polyimide membrane [6] showed non-ideal behaviour and significant polarization phenomena. For the completeness

of the experimental evidence it would be interesting to investigate the same liquid system for the rubbery PDMS polymer.

2. Experimental

2.1. Materials

Tetrahydrofuran (THF), *n*-hexane, *n*-heptane, toluene, isopropanol, ethanol, methanol and methyl ethyl ketone (MEK) (Merck) tetraoctylammonium bromide (Aldrich, The Netherlands) and the sunflower oil (Fluka, The Netherlands) were used as supplied, without further purification. The refined sunflower oil consisted of a mixture of triglycerides (mostly C_{18} with traces of C_{16} – C_{20} fatty acids), with molecular weight around 900 g mol^{-1} . Linoleic acid was the major component. Fig. 2a presents the chemical structures of sunflower oil and TOABr.

The PAN support membrane with MWCO of 30 kDa was provided by GKSS (Germany). The membrane was delivered in dry state and used without further treatment. The α,ω -dihydroxy PEO–PDMS–PEO block copolymer (ABA type, Q 3669, with PEO/PDMS content of 52/48%, w/w) was kindly supplied by Dow Corning (UK). Methacrylic anhydride (94%) was obtained from Aldrich (The Netherlands). The 4-dimethylaminopyridine (DMAP, 99%) was purchased from Fluka (The Netherlands) and the photo-initiator, Darocur 4265, was obtained from Ciba (The Netherlands). The PDMS (RTV 615 type, kindly supplied by General Electric, The Netherlands) was prepared at a pre-polymer/cross-linker ratio of 10/1.

2.2. Membrane preparation

Fig. 2b shows the structure of the α,ω -dihydroxy PEO–PDMS–PEO tri-block copolymer used in this study. In order to prepare a membrane, the copolymer should have cross-

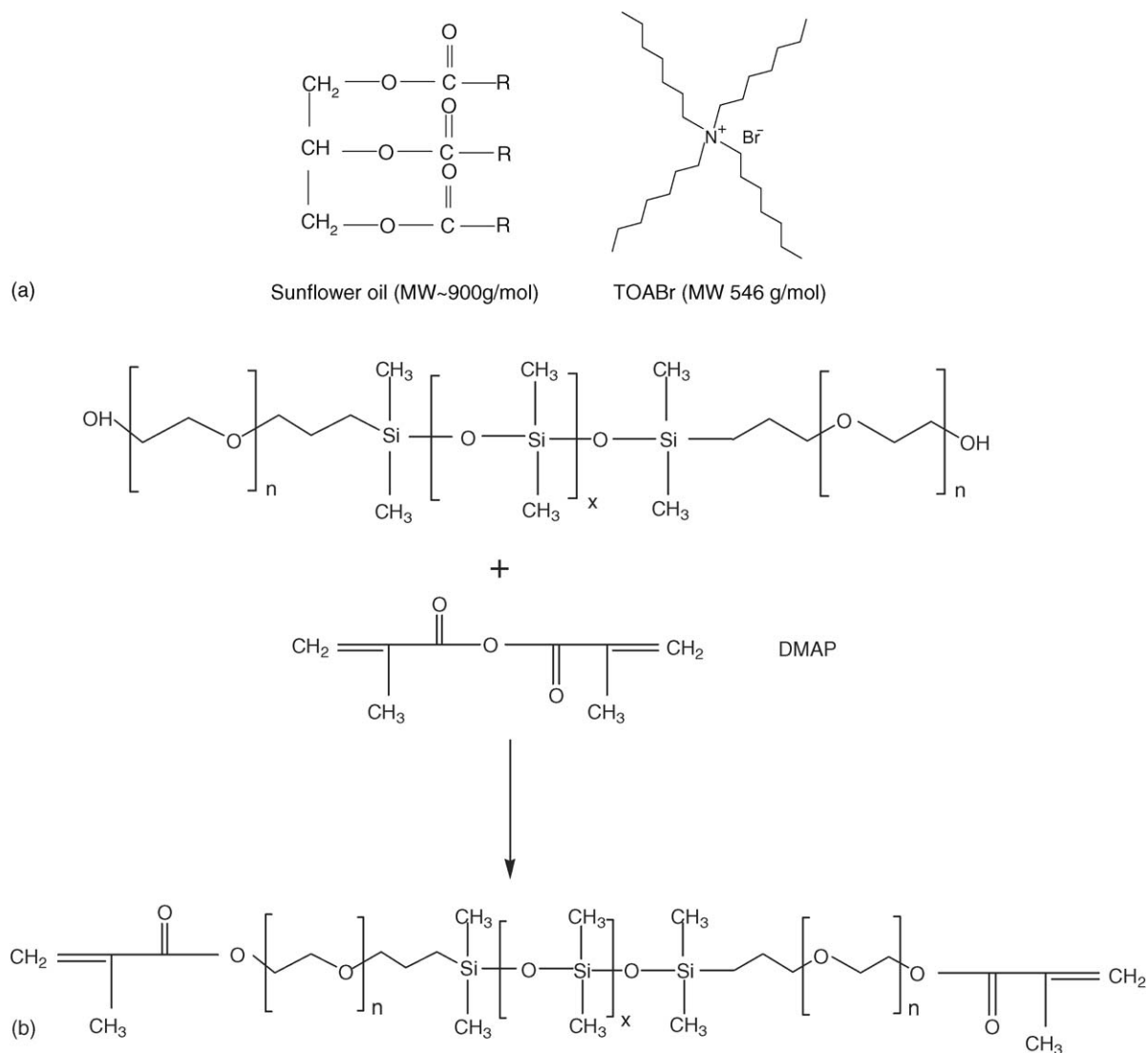


Fig. 2. (a) Chemical structures of sunflower oil and TOABr. (b) Synthesis of a UV-curable PEO–PDMS–PEO copolymer.

linkable functionality. Therefore, methacrylate (MA) functional groups were introduced which can be cross-linked by UV curing. The acylation reaction of α,ω -dihydroxy PEO–PDMS–PEO with methacrylic anhydride was conducted according to [8] (see Fig. 2b). The PEO–PDMS–PEO copolymer (18 g or 1×10^{-2} mol OH estimated) was stirred in a mixture of THF (90 ml) and DMAP (0.6 g or 4.9×10^{-3} mol) with an excess of methacrylic anhydride (6.4 g or 4×10^{-2} mol). The mixture was stirred for 72 h to assure complete conversion. The reaction mixture was concentrated on a rotary evaporator and precipitated in *n*-heptane (400 ml). Traces of *n*-heptane were removed under vacuum.

Free-standing, thick PEO–PDMS–PEO membranes were prepared by casting a mixture of the copolymer and photo-initiator on a glass plate, at room temperature (the photo-initiator is activated by UV light to form radicals which start the polymerization reaction). The glass plate was then placed in a UV-exposure chamber equipped with two Philips TLD 15/05 lamps (15 W, wavelength of 366 nm). The chamber was first flushed

with N_2 for 1 h (to remove oxygen) and then UV irradiation was performed for 2 h.

The PAN/PEO–PDMS–PEO composite membranes were prepared via dip-coating. The PAN support was glued on a glass plate with PVC tape and immersed in a vessel containing *n*-hexane to fill the pores. This was done to avoid pore intrusion of the PEO–PDMS–PEO during the dip coating process. Afterwards, the excess of hexane from the PAN surface was removed with a roller and the impregnated PAN support was dipped in a vessel containing the 20% (w/w) PEO–PDMS–PEO/methanol solution and the photo-initiator. The composite membrane was then placed in a UV-exposure chamber and the same UV-treatment as for the dense PEO–PDMS–PEO membrane was applied.

The PAN/PDMS free standing dense membranes and the tailor-made composite membranes were prepared following the procedure described elsewhere [2]. The selective PDMS top layer of the composite was prepared using a pre-polymer/cross-linker ratio of 10/1.

2.3. Membrane characterization

The characterization of the chemical composition of the PEO–PDMS–PEO membranes was performed by FTIR (Bio-Rad FS60). A GPC (Waters 515, using THF as solvent) was used to determine the MW of the copolymer before and after the acylation reaction. For the differential scanning calorimetry (DSC) measurements (Perkin-Elmer DSC 2 apparatus) the samples (1 mg) were scanned from -140 to 30 °C (heating rate: 30 °C min^{-1}). The contact angle of the membranes was measured by placing a small drop of water on the membrane with a syringe (Dataphysics Contact Angle System OCA 15 plus). A video camera recorded the drop, while the tangent at the point where the drop contacted the solid surface was calculated with SCA 20 software. Five drops of water were measured for each surface, and the average value was calculated.

For the swelling experiments, freestanding, thick PDMS and PEO–PDMS–PEO membranes were used following the procedure described elsewhere [2]. In the end of the experiments, the samples were removed from the liquid solutions and dried. From the difference between the initial and final dry weight, the concentration of the solute in the membrane ($c_{j,\text{membrane}}$) was measured and the solute partition coefficient K_j was calculated [2]. The membrane swelling is expressed as the volume fraction of solvent in the swollen polymer:

$$\phi_{\text{solvent}} = 1 - \frac{(1 - w_{\text{solvent}})/\rho_{\text{solvent}}}{(w_{\text{solvent}}/\rho_{\text{solvent}}) + (1 - w_{\text{solvent}}/\rho_{\text{polymer}})} \quad (1)$$

where w_{solvent} is the mass fraction of solvent in the swollen polymer, ρ_{polymer} the density of the PEO–PDMS–PEO (1.05 g cm^{-3} [9]) and ρ_{solvent} is the density of the solvent (taken from Ref. [10]).

2.4. Permeation set-up and analytical methods

All liquid permeation experiments were performed at 24 ± 3 °C using the dead-end filtration set-up and the protocol described in detail elsewhere [2]. Each permeation experiment was performed at least in triplicate. Values and error bars reported in the tables and figures are based on at least three different membranes.

The oil concentration in the feed and the permeate toluene solutions was analyzed by UV spectroscopy (Varian, Carry 300) at a wavelength of 295 nm. The concentration of TOABr was determined by gas chromatography (Shimadzu GC-2010 using a flame ionization detector and a Megabore column of diameter 0.32 mm and length 25 m). The viscosity of the solutions was measured using an Ubbelohde viscometer (model OC with an instrument coefficient of $0.0143 \times 10^{-6} \text{ m}^2 \text{ s}^{-2}$ ($0.0143 \text{ cSt s}^{-1}$)) obtained from Tomson, The Netherlands. The densities of the solutions were measured using a Digital Density Meter DMA 50, purchased from Anton Paar, The Netherlands.

3. Results and discussion

3.1. Characterization of the PEO–PDMS–PEO dense membrane

Fig. 3a shows a comparison of the FTIR spectra of PEO–PDMS–PEO copolymer, before and after the acylation reaction. Both spectra show similar peaks with the exceptions of the characteristic peak of the OH group at 3500 cm^{-1} (before acylation) and of the C=O group at 1720 – 1780 cm^{-1} (after acylation). The absence of the OH peak after acylation indicates the completeness of the acylation reaction. Fig. 3b presents a typical result of the GPC analysis for the PEO–PDMS–PEO copolymer before and after acylation. The results are similar, indicating that the reaction does not influence the MW of the copolymer. The GPC spectrum shows a peak of 3750 g mol^{-1} corresponding to the PEO–PDMS–PEO block copolymer and a peak of 850 g mol^{-1} probably indicating traces of low molecular weight polymer. From the GPC results and the composition of the copolymer given by the supplier (PEO/PDMS content of 52/48%, w/w), the MW of PEO and PDMS was estimated to be 975 and 1800 g mol^{-1} , respectively.

Fig. 3c shows the comparison of the FTIR spectra of the dense freestanding PEO–PDMS–PEO and PDMS membranes. Both spectra show the typical peaks of a silicone polymer: peak (a) corresponding to the $-\text{CH}_3$ stretch at 2965 cm^{-1} , peaks (c and e) corresponding to the Si– CH_3 bond at 1260 and 750 – 865 cm^{-1} , peak (d) corresponding to the broad polymer backbone band Si–O–Si between 1130 and 1000 cm^{-1} . The main difference between the spectra is the peak (b) corresponding to the C=O signal due to the incorporation of the MA group. The peak of the C–O bond from the PEO contribution at 1260 cm^{-1} might be masked by the higher intensity of the Si– CH_3 peak.

A typical DSC thermograph of the PEO–PDMS–PEO dense membrane shows a glass transition temperature (T_g) at about -80 °C which might correspond to the copolymer phase (note that T_g of PDMS is -123 °C and of PEO is between -115 and -40 °C, depending on the MW [9,10]) and a melting temperature (T_m) at -50 °C of the PDMS crystallites. The T_m of PDMS is rather close to the value reported in literature (range of -55 to -45 °C [10]).

3.2. Comparison between PDMS and PEO–PDMS–PEO membranes

Swelling experiments of the dense membranes were performed in hexane, toluene, MEK, isopropanol and ethanol (see Table 1). For the more hydrophilic PEO–PDMS–PEO membrane (contact angle, $\theta = 70 \pm 10^\circ$), the solvent fraction increases significantly with the polarity of the solvent, being the highest for ethanol. In contrary, for the hydrophobic PDMS membranes ($\theta = 105 \pm 8^\circ$), the highest swelling is found for the non-polar solvents such as hexane and toluene.

The flux of hexane, toluene, MEK, isopropanol and ethanol through the PAN/PDMS and PAN/PEO–PDMS–PEO composite membranes was measured at a transmembrane pressure of $30 \times 10^5 \text{ Pa}$ (30 bar). (The reader is reminded that no compaction

Table 1
Swelling of dense PEO–PDMS–PEO and PDMS membrane in various solvents

Solvent	Dielectric constant	Kinematic viscosity ($\times 10^{-6} \text{ m}^2 \text{ s}^{-1}$ (cSt))	$\phi_{\text{solvent, PEO–PDMS–PEO}}$	$\phi_{\text{solvent, PDMS}}$
Hexane	1.9	0.49	0.17 ± 0.02	0.77 ± 0.07
Toluene	2.4	0.66	0.20 ± 0.02	0.73 ± 0.08
MEK	15.4	0.53	0.51 ± 0.06	0.39 ± 0.04
Isopropanol	18.3	2.56	0.44 ± 0.03	0.30 ± 0.03
Ethanol	24.3	1.37	0.79 ± 0.06	0.11 ± 0.01

phenomena could be observed at these conditions.) Fig. 4 shows the effect of membrane swelling and solvent viscosity on solvent permeability (obtained by dividing the solvent flux through the membrane over the applied pressure). For both membranes a reasonably linear correlation exists between the solvent flux and $\phi_{\text{solvent}}/\eta_{\text{solvent}}$ (the R^2 is 0.86 for the PDMS membrane (Fig. 4a) and 0.90 for the PEO–PDMS–PEO (Fig. 4b)). For the PAN/PDMS membrane, the solvent permeability correlates better ($R^2 = 0.99$) with the $\phi_{\text{solvent}}/\eta_{\text{solvent}}$ if we consider MEK as an outlier (it is not known why MEK appears to have a special behaviour). For both composites in the given solvents and at the applied pressures, the results seem to be in line with our previous work [2] where we showed that normalization of the hexane permeability by the membrane swelling and the viscosity inside the membrane gives a unique constant value (interpreting the swelling as a measure for the solubility and the viscosity as a measure for the diffusion coefficient of the solvent inside the polymer). Similar conclusions have been reported by Vankelecom et al. [1] for the transport of various (polar and non-polar) solvents through a composite membrane consisting of PDMS as the selective layer and PAN/polyester (PE) as the support. The authors suggested that the viscosity could be regarded as a property reflecting the mutual interaction between the diffusing molecules and their interactions with the membrane and is influenced by the membrane swelling. Bhanushali et al. [4] corroborated the dependence of solvent permeability on its viscosity with the viscous (convective) flow. Robinson et al. [11] suggested that the swollen PDMS membrane might contain pores of Angstrom-dimension and identified the feed viscosity and membrane thickness as critical parameters controlling the mass transport. Currently, the transport mechanism in SRNF applications is one of the most discussed topics of investigation and debate. In this work, we will extend the experimental evidence by a systematic experimental protocol and qualitatively discuss the various parameters affecting solvent transport.

As expected, for the hydrophobic PAN/PDMS composite membrane the permeability of non-polar solvents (hexane, toluene) is significantly higher than the polar solvents (ethanol, isopropanol, see Fig. 4a). For the more hydrophilic PAN/PEO–PDMS–PEO membrane, the highest permeability is

observed for ethanol and MEK (see Fig. 4b). Similar behaviour has been reported for other silicone-based nanofiltration membranes, too [1,4,12–14]. Interestingly, the solvent permeability through the PAN/PEO–PDMS–PEO membrane is generally lower than the PAN/PDMS composite membrane, independent of the solvent nature. This may be due to either the quality of the composite membrane (effective top layer thickness and pore intrusion) or to the nature of the top layer. Concerning the quality of the composite, in earlier work for the PAN/PDMS composite membranes [7] we found that the polymer pore intrusion may restrict the PDMS swelling and cause a lowering of the membrane permeability. Concerning the polymer nature, the PEO might be less permeable material than PDMS. To get some indication one can turn to the gas permeation properties of the materials. The PDMS homo-polymer, has high intrinsic CO_2 permeability ($2.4 \times 10^{-10} \text{ cm}^3(\text{STP}) \text{ cm cm}^{-2} \text{ s}^{-1} \text{ Pa}^{-1}$) [10]. The intrinsic CO_2 permeability of the PEO homo-polymer is however much lower ($0.1 \times 10^{-10} \text{ cm}^3(\text{STP}) \text{ cm cm}^{-2} \text{ s}^{-1} \text{ Pa}^{-1}$, estimated at 35°C) [15]. Therefore, a lower CO_2 permeability should be expected for the PEO–PDMS–PEO copolymer than for the PDMS polymer. Table 2 presents the gas permeation results of the composite membranes which confirm our expectations. For the PAN/PEO–PDMS–PEO composite membrane, the N_2 and CO_2 permeabilities are much lower than through the PAN/PDMS.

3.3. Transport through the PAN/PDMS composite membrane

In this section, a systematic study of the transport through the PAN/PDMS membrane is presented. The results are compared with earlier findings for the transport of oil/hexane mixtures through the same membrane [2]. Fig. 5 presents the kinematic viscosities of the various solutions. The viscosity of the oil/solvent mixtures increases with the oil concentration (see inset of Fig. 5). However, the viscosity of TOABr/toluene solution increases much with the TOABr concentration in agreement with results reported by Peeva et al. [6]. The significant increase of solution viscosity with the TOABr concentration may be due to the self-association of TOABr in ion-pair clusters [16,17].

Table 2
Gas transport properties of the PAN/PEO–PDMS–PEO and PAN/PDMS composite membranes

Membrane	$(P/l)_{\text{N}_2}$ ($\times 10^{-10} \text{ cm}^3(\text{STP}) \text{ cm}^{-2} \text{ s}^{-1} \text{ Pa}^{-1}$)	$(P/l)_{\text{CO}_2}$ ($\times 10^{-10} \text{ cm}^3(\text{STP}) \text{ cm}^{-2} \text{ s}^{-1} \text{ Pa}^{-1}$)	$\alpha_{\text{CO}_2/\text{N}_2}$
PAN/PEO–PDMS–PEO	2.3 ± 0.8	31 ± 5	13.7 ± 1.9
PAN/PDMS	120 ± 17	1282 ± 180	9.8 ± 1.4

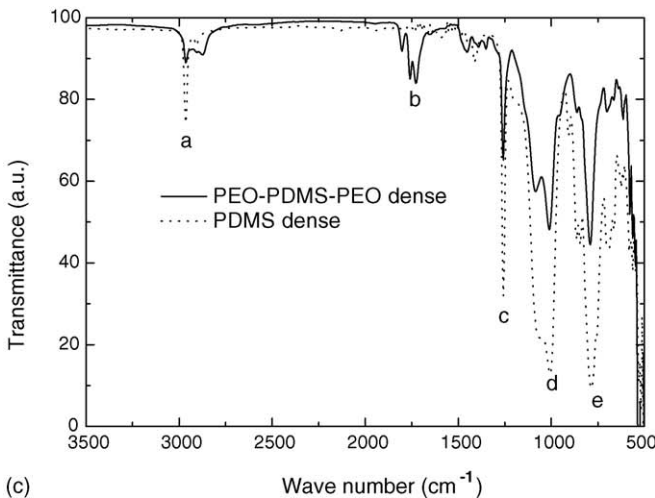
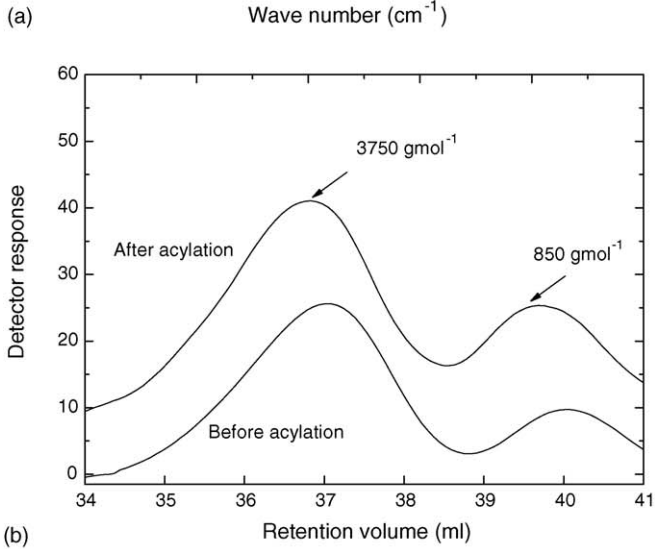
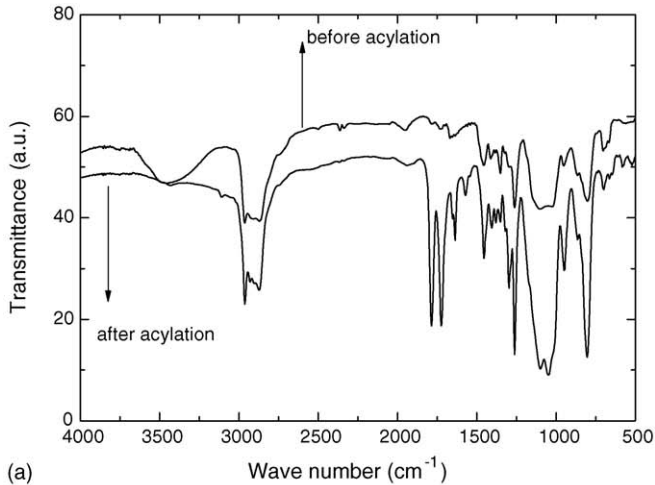


Fig. 3. (a) FTIR spectra of the PEO-PDMS-PEO copolymer. (b) The MW of the PEO-PDMS-PEO copolymer determined by GPC. (c) FTIR spectra of the dense PEO-PDMS-PEO and PDMS membranes.

3.3.1. Sunflower oil/toluene mixtures

Fig. 6 presents the solvent volume fraction (ϕ_{solvent}) in the membrane at various oil/toluene concentrations. For comparison, the data obtained for the oil/hexane system are presented, too [2]. The membrane swelling in pure toluene is high, as

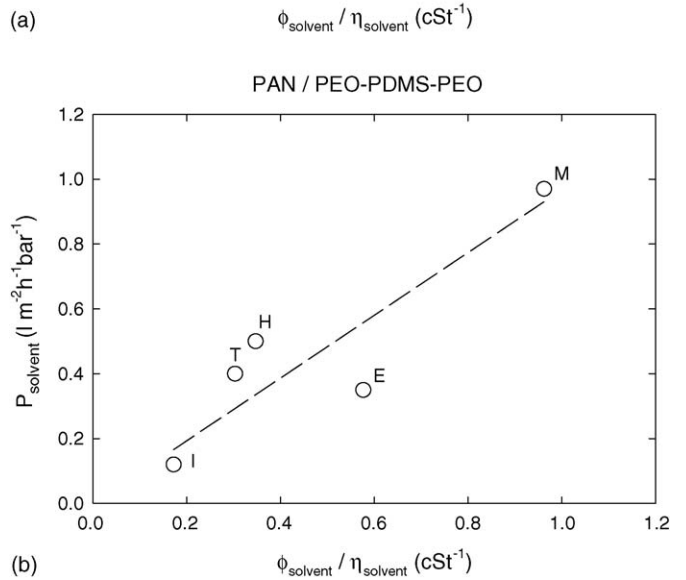
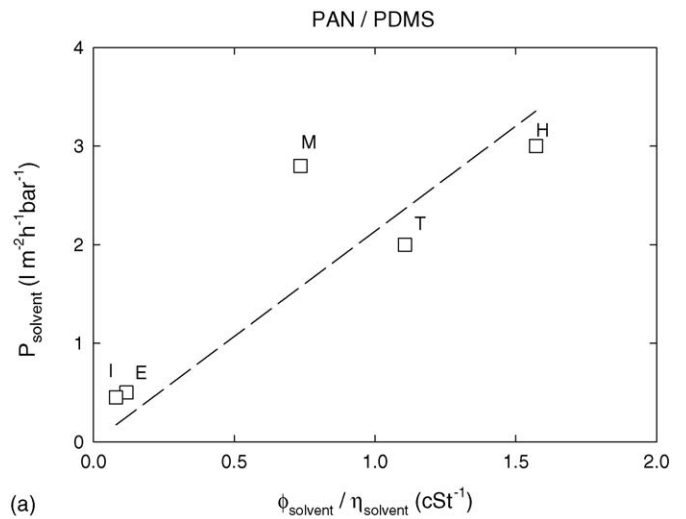


Fig. 4. Solvent permeability at 30×10^5 Pa (30 bar) through (a) PAN/PDMS and (b) PAN/PEO-PDMS-PEO membrane as a function of membrane swelling (ϕ_{solvent}) and solvent viscosity (η_{solvent}). E: ethanol, M: MEK, T: toluene, H: hexane, I: isopropanol.

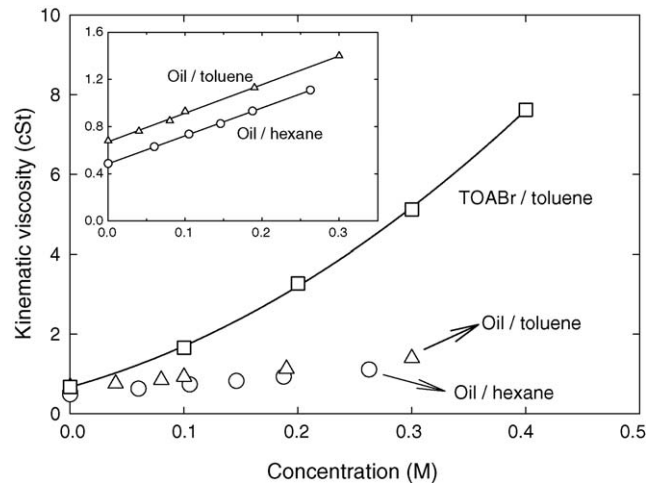


Fig. 5. Kinematic viscosity of the mixtures used in this study. Inset: oil/solvent mixtures.

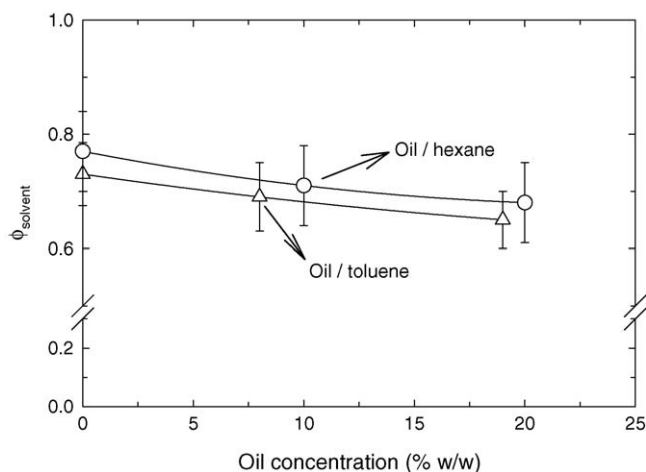


Fig. 6. Effect of oil concentration on the solvent volume fraction inside the membrane.

Table 3

Flory–Huggins interaction parameter (χ) calculated from the swelling experiments

Penetrant	$\chi_{\text{PDMS-penetrant}}$
Toluene	0.61 ± 0.02
Hexane ^a	0.58 ± 0.03
Oil ^a	2.11 ± 0.02

^a Results from Ref. [2].

expected from their similar solubility parameters ($\delta_{\text{toluene}} = 18.2$ and $\delta_{\text{PDMS}} = 14.9\text{--}15.6 \text{ MPa}^{1/2}$ [10]) and decreases with the increase of oil concentration (being very low, about 5%, in pure oil [2]). Table 3 presents the results of the χ interaction parameter for toluene, hexane and oil calculated using the Flory–Huggins solution theory (more details concerning the calculation are presented in Ref. [2]). For pure toluene, χ is about 0.6 indicating a good membrane–toluene interaction whereas for the oil a χ value of 2.1 indicates low interaction with the membrane. When toluene and hexane are compared, the interaction parameter between PDMS–solvent is similar.

Table 4 presents the concentration of oil in swollen PDMS membrane and the oil partition coefficients, K_{oil} , at various oil/toluene concentrations. For comparison, the data reported for the oil/hexane system [2] are presented too. The K_{oil} is generally lower for the 19% (w/w) mixtures but the values for the 8

Table 4
Oil concentration and partition coefficient inside dense PDMS membrane

Solution	Oil concentration (% w/w)	$C_{\text{oil, membrane}} (\%, \text{ w/w})$	K_{oil}
Oil/toluene	8	4.1 ± 0.2	0.51 ± 0.02
	19	8.3 ± 1.0	0.44 ± 0.06
Oil/hexane ^a	8	4.7 ± 0.3	0.59 ± 0.02
	19	8.1 ± 0.6	0.43 ± 0.04

^a Results from Ref. [2].

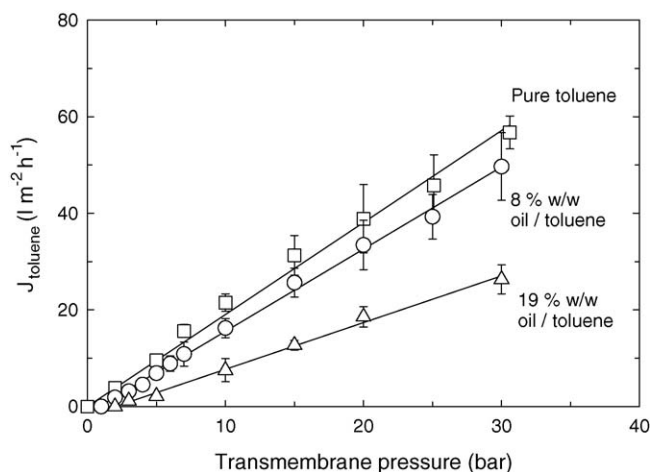


Fig. 7. Toluene flux through PAN/PDMS composite membrane as a function of the transmembrane pressure at various oil/toluene concentrations.

19% (w/w) solutions are similar for oil/toluene and oil/hexane solutions.

The permeation performance of the PAN/PDMS composite membrane in oil/toluene solutions at various concentrations was systematically investigated. First, the performance of the PAN/PDMS composite membrane at high pressure and long permeation time was investigated. The toluene flux through the PAN/PDMS membrane stays constant for several hours at various transmembrane pressures. In addition, no flux hysteresis with the applied pressure was found, showing that probably the applied pressure does not affect the membrane structure (results not shown here). Fig. 7 presents the effect of the transmembrane pressure on the toluene flux (J_{toluene}) at various oil/toluene concentrations. The linearity of J_{toluene} with applied pressure indicates that no compaction of the membrane occurs over the applied pressure range. The pure solvent permeability, P (calculated from the slope of the J_{toluene} versus Δp plot) is $2.0 \pm 0.3 \times 10^{-5} \text{ l m}^{-2} \text{ h}^{-1} \text{ Pa}^{-1}$ ($2.0 \pm 0.3 \text{ l m}^{-2} \text{ h}^{-1} \text{ bar}^{-1}$) for toluene (and $3.0 \pm 0.4 \times 10^{-5} \text{ l m}^{-2} \text{ h}^{-1} \text{ Pa}^{-1}$ ($3.0 \pm 0.4 \text{ l m}^{-2} \text{ h}^{-1} \text{ bar}^{-1}$) for hexane [2]). Since the swelling of the membrane is similar for the two solvents (see Fig. 6), the difference in permeability should probably be attributed to differences in viscosity. Table 5 shows that when the apparent solvent permeability is normalized for the membrane swelling and viscosity, the same value is obtained for both solvents, consistent with the results of Fig. 4. The toluene permeability reported for other silicone type NF composites are: $1.2 \times 10^{-5} \text{ l m}^{-2} \text{ h}^{-1} \text{ Pa}^{-1}$ ($1.2 \text{ l m}^{-2} \text{ h}^{-1} \text{ bar}^{-1}$) for PAN–PE/PDMS membrane [1], $1.3 \times 10^{-5} \text{ l m}^{-2} \text{ h}^{-1} \text{ Pa}^{-1}$ ($1.3 \text{ l m}^{-2} \text{ h}^{-1} \text{ bar}^{-1}$) for the MPF-50 membrane [14] and $0.4 \times 10^{-5} \text{ l m}^{-2} \text{ h}^{-1} \text{ Pa}^{-1}$ ($0.4 \text{ l m}^{-2} \text{ h}^{-1} \text{ bar}^{-1}$) for our PAN/PEO–PDMS–PEO composite (see Fig. 4b). For comparison, the toluene permeability through some non-silicone NF membranes: $0.6 \times 10^{-5} \text{ l m}^{-2} \text{ h}^{-1} \text{ Pa}^{-1}$ ($0.6 \text{ l m}^{-2} \text{ h}^{-1} \text{ bar}^{-1}$) for a polyamide type membrane (Desal 5, Osmonics) [4] and $1.8 \times 10^{-5} \text{ l m}^{-2} \text{ h}^{-1} \text{ Pa}^{-1}$ ($1.8 \text{ l m}^{-2} \text{ h}^{-1} \text{ bar}^{-1}$) for a polyimide membrane (STARMEMTM 122) [6].

Table 5
Parameters concerning the transport through the PAN/PDMS composite membranes

Solvent	Oil concentration (%, w/w)	$\eta_{\text{apparent}} (\times 10^{-6} \text{ m}^2 \text{ s}^{-1} \text{ (cSt)})$	$P_{\text{solvent}} (\times 10^{-5} \text{ l m}^{-2} \text{ h}^{-1} \text{ Pa}^{-1})$ ($\text{l m}^{-2} \text{ h}^{-1} \text{ bar}^{-1}$)	ϕ_{solvent}	$P\eta_{\text{apparent}}/\phi_{\text{solvent}}$ ($\times 10^{-11} \text{ l m}^2 \text{ s}^{-1} \text{ m}^{-2} \text{ h}^{-1} \text{ Pa}^{-1}$) ($\text{l cSt m}^{-2} \text{ h}^{-1} \text{ bar}^{-1}$)
Toluene	0	0.61 ± 0.02	2.0 ± 0.3	0.73 ± 0.07	1.7 ± 0.2
	8	0.72 ± 0.01	1.6 ± 0.2	0.70 ± 0.06	1.6 ± 0.2
	19	0.89 ± 0.01	1.1 ± 0.2	0.64 ± 0.07	1.5 ± 0.2
Hexane ^a	0	0.48 ± 0.02	3.0 ± 0.4	0.77 ± 0.08	1.8 ± 0.3
	8	0.57 ± 0.01	2.3 ± 0.3	0.73 ± 0.06	1.8 ± 0.3
	19	0.63 ± 0.01	1.7 ± 0.4	0.69 ± 0.07	1.6 ± 0.2

^a Results from Ref. [2].

In Fig. 7, the x -intercepts (at $J_{\text{toluene}} = 0$) for each oil/toluene concentration can be compared with the osmotic pressures, $\Delta\pi$, calculated using the van't Hoff equation:

$$\Delta\pi = \frac{R_g T \Delta c}{MW} \quad (2)$$

Δc is the solute concentration difference across the membrane and MW is the solute molecular weight. The van't Hoff equation is applicable in oil/toluene solutions due to the relative low feed concentrations (0.08 – 0.18 mol l^{-1}). The x -intercept seems to be in good agreement with the $\Delta\pi$ estimated by Eq. (2) (x -intercept/calculated $\Delta\pi$ value: for 8% (w/w), $1.1 \times 10^5 \text{ Pa}/1.3 \times 10^5 \text{ Pa}$ ($1.1 \text{ bar}/1.3 \text{ bar}$), for 19% (w/w), $2.2 \times 10^5 \text{ Pa}/2.6 \times 10^5 \text{ Pa}$ ($2.2 \text{ bar}/2.6 \text{ bar}$)). Similarly, good agreement was found earlier [2] for the oil/hexane system. It seems that oil/toluene and oil/hexane behave ideally and (as it happens for aqueous systems) the van't Hoff osmotic pressure model can interpret them well.

The toluene permeability coefficient at various feed concentrations (calculated from the slopes of the graphs of Fig. 7) decreases with oil concentration (see Table 4). For oil/hexane solutions, we reported earlier [2] that the main parameters affecting the hexane permeability through the PAN/PDMS were the “apparent” viscosity inside the membrane and the membrane swelling. Similarly, for the oil/toluene system, the “apparent” viscosity inside the membrane is estimated from the concentration of oil in an hypothetical oil/toluene phase inside the membrane for the dense PDMS membranes (results of Table 5) and the plots of viscosity versus oil/toluene (see Fig. 5). For the swelling, the results of Fig. 6 concerning the dense PDMS membranes are used. Table 5 shows that for various oil/toluene concentrations, the normalized toluene permeabilities do not differ, significantly.

In earlier work [2,7], we studied the transport of oil/hexane and poly isobutylene/hexane mixtures (PIB of MW 350 and 1300) through the PAN/PDMS membrane. At the same solute/hexane concentration (8%, w/w), the coupling and dragging was more significant for the PIB of the lowest molecular weight: 350 (PIB 350, see Fig. 8). In these systems, the membrane swelling and the apparent viscosity inside the membrane were comparable and therefore the higher dragging of PIB 350 was attributed to its higher partition inside the mem-

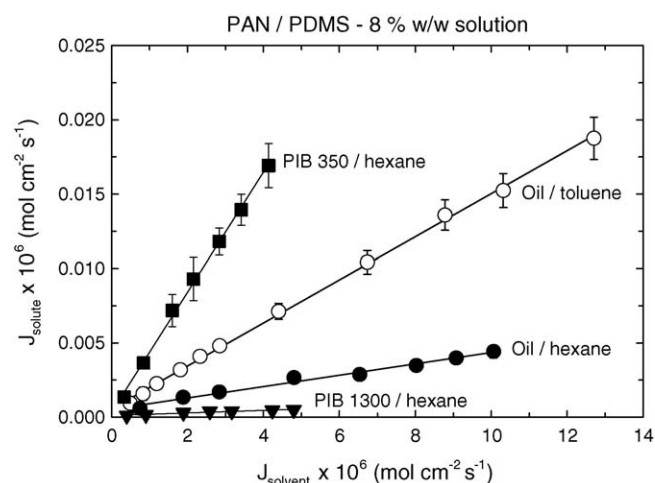


Fig. 8. Solute flux as a function of the solvent flux.

brane ($K_{\text{PIB 350}} = 0.88$, $K_{\text{oil}} = 0.59$ and $K_{\text{PIB 1300}} = 0.53$ [7,18]¹). At high oil/hexane concentrations (19 and 30%, w/w), however, the dragging of oil by the hexane was found to decrease [2]. This was correlated with the decrease of the membrane swelling and of K_{oil} as well as the increase of the apparent viscosity inside the membrane, at high oil/hexane concentrations. All these factors seem to lead to restriction of dragging of oil by the hexane.

For the oil/toluene mixtures, the coupling seems to be more significant than for the oil/hexane system (see comparison in Fig. 8) although the concentration of oil inside the membrane (Table 4) and the membrane swelling are comparable (Table 5). In both cases extrapolation towards zero solvent flux representing in fact a diffusion experiment gives extremely low transport rates of oil ($\sim 5.5 \times 10^{-10} \text{ mol cm}^{-2} \text{ s}^{-1}$). The higher coupling of oil by toluene might be due to the generally high viscosity of oil/toluene solutions (30–40% higher than the oil/hexane solution, see Table 5). The viscosity of pure toluene is higher than of pure hexane. Furthermore, one can argue that the oil despite the presence of the bulky R-groups has a somewhat polar character due to the presence of ester groups (see Fig. 2a). This

¹ The reader should note that the partition coefficients of PIB 350 and 1300 into PDMS have not been reported correctly in Ref [2]. However, the errors have been corrected in Refs. [7,18].

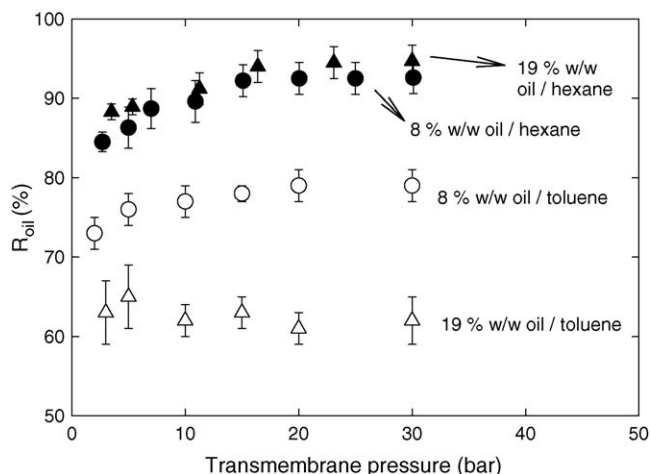


Fig. 9. Oil retention by the PAN/PDMS composite membrane as a function of transmembrane pressure for various mixtures.

might result to better solvation of oil in toluene than in hexane and therefore to higher coupling and dragging. Fig. 9 shows the effect of transmembrane pressure on membrane retention at various oil/toluene solutions. For 8% (w/w) solution, the membrane retention somewhat increases with the applied pressure (from 73 to 79%). For 19% (w/w) oil/toluene solution, the membrane retention does not change with the transmembrane pressure and it is lower compared to the 8% (w/w) solution. The latter is probably due to the increased driving force (concentration difference) for the oil transport and the increased dragging by toluene due to further increase of viscosity at high oil/toluene concentrations. In comparison to oil/hexane system, the retention for the oil/toluene is generally lower (see Fig. 9) probably due to the increased dragging of oil by the toluene.

3.3.2. TOABr/toluene mixtures

The results for the oil/toluene mixtures seem to be rather similar with those of oil/hexane [2]. The TOABr/toluene mixture, however, is expected to be more complex. In this case, the viscosity increases significantly with concentration (Fig. 5) and Peeva et al. [6] reported non-ideal behaviour and significant concentration polarization phenomena.

Figs. 10 and 11 present the effect of transmembrane pressure on toluene flux through the PAN/PDMS composite membrane, at various TOABr/toluene concentrations. For both 8 and 19% (w/w) solutions the trends are the same. At low pressures, the toluene flux increases almost linearly with pressure and reaches a plateau. These results indicate significant polarization phenomena in agreement with the observations of Peeva et al. [6] and are markedly different from those of oil/toluene solution (see comparison in Figs. 10 and 11). At high pressures, the increase of TOABr concentration at the feed side of the membrane and the consequent increase of solution viscosity cause a significant decrease of toluene flux through the membrane. The polarization phenomena are probably due to formation of TOABr dimeric or oligomer ion-pairs in toluene due to its specific chemical structure (Fig. 2a). The TOABr oligomerization in various organic solvents, including toluene, has already been reported in litera-

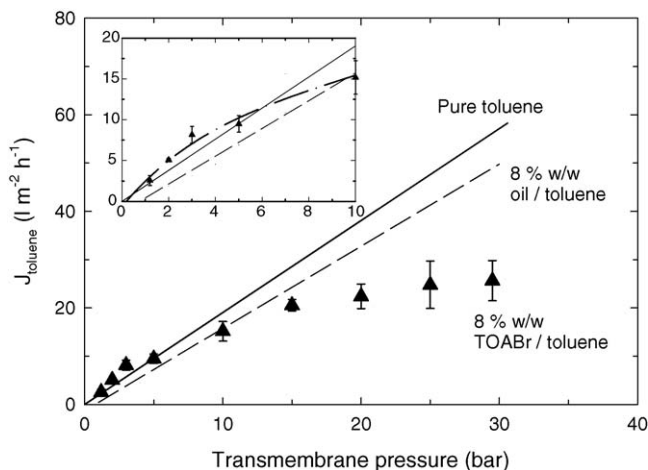


Fig. 10. Toluene flux as a function of transmembrane pressure for the 8% (w/w) solute/toluene mixtures. Inset: zoom at low pressures.

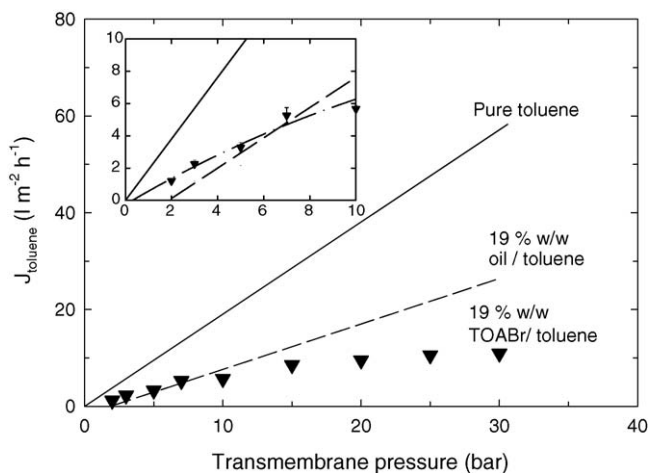


Fig. 11. Toluene flux as a function of transmembrane pressure for the 19% (w/w) solute/toluene mixtures. Inset: zoom at low pressures.

ture [16,17] and can explain the significant increase of solution viscosity at high TOABr concentrations. Besides, it is important to note that attempts to measure the partition of TOABr into dense PDMS membranes were not successful. Due to the high solution viscosity, a layer of TOABr was deposited on the PDMS surface (which was often very difficult to remove) and introduced large errors to the measurements.

Furthermore for the TOABr/toluene mixture, the osmotic phenomena are significantly lower than for the ideal oil/toluene solutions. Table 6 shows that the x -intercepts of the plots of toluene flux versus transmembrane pressure are significantly lower than the osmotic pressure calculated by van't Hoff (see

Table 6

Comparison between the $\Delta\pi$ calculated by the van't Hoff equation and the x -intercepts of the plots of J_{toluene} vs. transmembrane pressure (Figs. 10 and 11)

TOABr concentration (% w/w)	$\Delta\pi_{\text{calculated}}$ ($\times 10^5$ Pa (bar))	x -Intercept ($\times 10^5$ Pa (bar))
8	3.0	0.3
19	8.0	0.5

insets in Figs. 10 and 11). The reasons for this behaviour could be (i) the non-ideality of the TOABr/toluene system; Peeva et al. [6] showed that an activity coefficient (γ) as low as 1.1 can almost let the osmotic pressure vanish and/or (ii) the formation of TOABr dimeric or polymeric species in toluene; this causes a decrease of the “effective” TOABr concentration and increase of their molecular weight. Both changes can decrease the apparent osmotic pressure of the solution (see Eq. (2)).

Finally, the membrane retention for TOABr is almost 100% at all pressures and feed concentrations. This can also be correlated to the formation of TOABr oligomer species and the significant concentration polarization phenomena which cause reduction of toluene flux and 100% retention of TOABr by the membrane. Similar results were obtained by Peeva et al. [6] for the STARMEM polyimide membrane (membrane retention: 99%).

4. Conclusions

This work presented a systematic investigation of various SRNF systems. First, a comparison between the permeation performance of various solvents through a hydrophilic and a hydrophobic PDMS-based composite membrane was studied. Then, the transport of oil/toluene and TOABr/toluene mixtures through the PAN/PDMS composite membranes was investigated. The main conclusions are:

- The permeability of pure solvents (polar or non-polar) through the hydrophobic PAN/PDMS and the more hydrophilic PAN/PEO–PDMS–PEO seems to be generally dependent on the membrane swelling and the solvent viscosity.
- The oil/toluene system is ideal. The observed osmotic phenomena can be interpreted with the van't Hoff osmotic model. The “apparent” viscosity inside the membrane and the membrane swelling govern the toluene transport through the PAN/PDMS composite membrane. The flux coupling for oil–toluene seems to be more significant than for oil–hexane probably due to the higher viscosity of the oil/toluene solutions.
- The TOABr/toluene system is non-ideal. The osmotic pressure was significantly lower than expected based on the van't Hoff model. Due to the ion-pair clustering of TOABr in toluene concentration polarization phenomena are observed resulting in low toluene flux and 100% retention of TOABr by the PAN/PDMS composite membrane.

Acknowledgements

The CW/STW, Shell Global Solution (Amsterdam), Akzo Nobel Chemicals Research (Arnhem), Nederlandse Organisatie voor Toegepast Natuurwetenschappelijk Onderzoek Divisie Materiaaltechnologie (Eindhoven), Solsep B.V. Robust Separation Technologies (Apeldoorn) and DSM-Research CT&A (Geleen) are gratefully acknowledged for the financial support of this work (project number 790.35.249).

The authors wish to thank: G.-H. Koops and H. Zwijnenberg (European Membrane Membrane Institute—Twente, University

of Twente, The Netherlands), A. Nijmeijer (Shell Global Solution), G. Bargeman (Akzo Nobel Chemicals Research), F.P. Cuperus (Solsep B.V. Robust Separation Technologies) and J. Krijgsman (DSM-Research CT&A) for the fruitful discussions and C.J. Padberg (Materials Science and Technology of Polymers Group, University of Twente, The Netherlands) for his assistance with the GPC and DSC analysis.

References

- [1] I.F.J. Vankelecom, K. De Smet, L.E.M. Gevers, A. Livingston, D. Nair, S. Aerts, S. Kuypers, P.A. Jacobs, Physico-chemical interpretation of the SRNF transport mechanism for solvents through dense silicone membranes, *J. Membr. Sci.* 231 (2004) 99–108.
- [2] N. Stafie, D.F. Stamatialis, M. Wessling, Insight into the transport of hexane–solute systems through tailor-made composite membranes, *J. Membr. Sci.* 228 (2004) 103–116.
- [3] G.H. Koops, S. Yamada, S.-I. Nakao, Separation of linear hydrocarbons and carboxylic acids from ethanol and hexane solutions by reverse osmosis, *J. Membr. Sci.* 189 (2001) 241–254.
- [4] D. Bhanushali, S. Kloos, D. Bhattacharyya, Solute transport in solvent-resistant nanofiltration membranes for non-aqueous systems: experimental results and the role of solute–solvent coupling, *J. Membr. Sci.* 208 (2002) 343–359.
- [5] J.T. Scarpello, D. Nair, L.M. Freitas dos Santos, L.S. White, A.G. Livingston, The separation of homogeneous organometallic catalysts using solvent resistant nanofiltration, *J. Membr. Sci.* 203 (2002) 71–85.
- [6] L.G. Peeva, E. Gibbins, S.S. Luthra, L.S. White, R.P. Stateva, A.G. Livingston, Effect of concentration polarisation and osmotic pressure on flux in organic solvent nanofiltration, *J. Membr. Sci.* 236 (2004) 121–136.
- [7] N. Stafie, D.F. Stamatialis, M. Wessling, Effect of cross-linking degree of PDMS on the permeation performance of PAN/PDMS composite nanofiltration membranes, *Sep. Purif. Technol.* 45 (2005) 220–231.
- [8] G. Höfl, W. Steglich, H. Vorbruggen, 4-Dialkylaminopyridine als hochwirksame Acylierungskatalysatoren, *Angew. Chem.* 90 (1978) 602–615.
- [9] Z.-R. Zhang, M. Gottlieb, Amphiphilic poly(ethylene oxide)/poly(dimethylsiloxane) polymers 1. Synthesis and characterization of cross-linked hydrogels, *Thermochim. Acta* 336 (1999) 133–145.
- [10] J. Brandrup, E.H. Immergut, *Polymer Handbook*, second ed., Wiley Interscience, 1975.
- [11] J.P. Robinson, E.S. Tarleton, C.R. Millington, A. Nijmeijer, Solvent flux through dense polymeric nanofiltration membranes, *J. Membr. Sci.* 230 (2004) 29–37.
- [12] D.R. Machado, D. Hasson, R. Semiat, Effect of solvent properties on permeate flow through nanofiltration membranes. Part I: investigation of parameters affecting solvent flux, *J. Membr. Sci.* 163 (1999) 93–102.
- [13] D. Bhanushali, S. Kloos, C. Kurth, D. Bhattacharyya, Performance of solvent-resistant membranes for non-aqueous systems: solvent permeation results and modeling, *J. Membr. Sci.* 189 (2001) 1–21.
- [14] X.J. Yang, A.G. Livingston, L.M. Freitas dos Santos, Experimental observations of nanofiltration with organic solvents, *J. Membr. Sci.* 190 (2001) 45–55.
- [15] H. Lin, B.D. Freeman, Gas solubility, diffusivity and permeability in poly(ethylene oxide), *J. Membr. Sci.* 239 (2004).
- [16] K. Sawada, E. Takahashi, T. Horie, K. Satoh, Solvent effects on ion-pair distribution and dimerization of tetraalkylammonium salts, *Monats. fur Chem.* 132 (2001) 1439–1450.
- [17] C. Klofutar, S. Paljk, Aggregation of tri-*n*-octylammonium chloride (TOACHCl), tri-*n*-octylammonium bromide (TOAHBr) and tri-*n*-octylammonium iodide (TOAHI) in benzene solutions, *Inorg. Chim. Acta* 40 (1980) 167.
- [18] N. Stafie, Poly(dimethyl siloxane) based composite nanofiltration membranes for non aqueous applications, Ph.D. thesis, University of Twente, 2004.